Available online at www.sciencedirect.com

ScienceDirect

Ceramics International 40 (2014) 1297–1302

CERAMICS INTERNATIONAL

www.elsevier.com/locate/ceramint

Titania nanotubes and fullerenes C_{60} assemblies and their photocatalytic activity under visible light

Mathieu Grandcolas[a,*], Jinhua Ye[b,**], Kunichi Miyazawa[c]

[a]International Center for Young Scientists (ICYS), Tsukuba, Ibaraki 305-0047, Japan
[b]Photocatalytic Material Center, National Institute for Materials Science (NIMS), 1-2-1 Sengen, Tsukuba, Ibaraki 305-0047, Japan
[c]Fullerene Engineering, Advanced Nano Materials Laboratory, National Institute for Materials Science, 1-1 Namiki, Tsukuba, Ibaraki 305-0044, Japan

Received 28 March 2013; accepted 1 July 2013
Available online 6 July 2013

Abstract

Titania nanotubes (TiNTs) functionalized with fullerenes (C_{60}) have been successfully synthesized through a simple impregnation method using ethanol and toluene as co-solvents. The as-synthesized samples were characterized by X-ray diffraction (XRD), scanning and transmission electron microscopy (SEM, TEM), Raman spectroscopy, and UV–vis spectroscopy. Differences in UV–vis light absorption of TiNTs samples loaded with 1%, 2% and 5% C_{60} were attributed to excited states from the formation of fullerene aggregates. C_{60}-sensitizing was found to effectively enhance the photocatalytic degradation of an organic molecule in the gas phase. Photocatalytic decomposition of isopropanol was carried out and showed high degradation in the visible region, where the TiNTs samples loaded with 5 wt% C_{60} offered the best activity.

Keywords: Titania nanotubes; Fullerene; Heterogeneous photocatalysis; Visible light

1. Introduction

The efficient utilization of solar energy is one of the major goals of modern science and engineering. Among all the materials being developed for photocatalytic applications, titanium dioxide (TiO_2) and their related materials are the most promising because of their high efficiency, low cost, chemical inertness and high photostability [1]. One-dimensional photocatalysts, especially titania nanotubes (TiNTs), are attracting extensive research interest due to useful properties like cation exchange [2], electrochromism [3], photoinduced hydrophilicity [4], and degradation of hazardous chemicals [5]. Different methods exist for the preparation of TiNTs such as use of a anodic aluminum oxide (AAO) or carbon nanotube (CNT) template [6,7], the hydrogel route [8], and anodization [9]. However, the most convenient method for large scale synthesis of TiNTs is the hydrothermal route [10]. Several different structures have been proposed including scrolling of anatase TiO_2 sheets [11], lepidocrocite $H_xTi_{2-x/4}\square_{x/4}O_4$ ($x\sim0.7$, $\square$: hole) [12], trititanate $H_2Ti_3O_7$ exfoliated sheets [13], and $(Na,H)_2Ti_2O_4(OH)_2$-based layers [14], although the exact composition is still under discussion and seems strongly dependent on the synthesis method. Unfortunately, for visible light applications, TiNTs exhibit a large band gap around 3.5 eV, which is even larger than the ~3.1 eV band gap found for TiO_2 anatase. In order to shift the absorption capability of TiNTs, different techniques have been explored in the literature such as doping [15], composite formation with another semiconductor [16], and polymeric sensitizing [17]. Dye sensitization is also an efficient way to expand the absorption range of a semiconductor, and has been utilized in solar cells [18] and for visible light induced photocatalysis [19].

Carbonaceous composites (granular or fiber activated carbon, graphene, CNTs, etc.) with TiO_2 have recently attracted considerable attention [20,21]. Some studies have shown that CNTs exhibit a synergic effect in enhancing the photocatalytic activity of TiO_2 through electron transfer from TiO_2 to CNTs. The direct band gap of solid fullerenes C_{60} is found to be 1.6–1.9 eV between the highest occupied molecular orbital (HOMO) and the lowest unoccupied molecular orbital (LUMO) [22], which gives

*Corresponding author. Tel.: +47 934 01 418.
**Corresponding author. Tel.:+81 29 859 2646.
E-mail addresses: grandcolasm@gmail.com (M. Grandcolas), jinhua.ye@nims.go.jp (J. Ye).

0272-8842/$ - see front matter © 2013 Elsevier Ltd and Techna Group S.r.l. All rights reserved.
http://dx.doi.org/10.1016/j.ceramint.2013.07.009

rise to an absorption window ranging from the UV to the near IR and makes it an attractive option for photocatalytic applications in the visible range. Kamat reported the first photoinduced charge transfer between a semiconductor (ZnO) and a carbon cluster (C_{60} and C_{70}). Using different techniques like laser flash photolysis and infrared spectroscopy FT-IR, photoinduced charge transfer was demonstrated between C_{60} and TiO_2 [23]. Later, Makarov et al. showed that a TiO_2–C_{60} multilayer structure was photosensitive through measured changes in the fullerene layer conductivity [24]. Overall, fullerenes present a unique three-dimensional structure with delocalized π electrons which may act as a sensitizer when attached to the surface of a photocatalyst, thus enabling a participatory role in the surface photochemical processes.

In total, we report here a simple method for C_{60}-sensitized TiNTs synthesis, with a focus on characterization of the effects of C_{60} concentration on TiNTs using an organic solvent impregnation process. The attachment of C_{60} species onto TiNTs was evaluated by transmission electron microscope (TEM) and energy dispersive spectroscopy. Its photocatalytic activity towards an organic molecule mineralization under visible light radiation is investigated.

2. Materials and methods

2.1. Photocatalyst preparation

TiNTs were synthesized via a hydrothermal reaction of commercial TiO_2 powder in concentrated sodium hydroxide (NaOH) [11]. First, 4 g of TiO_2 nanoparticles (25 nm, anatase, Aldrich) was mixed with 200 mL of 10 M NaOH in a Teflon autoclave and stirred for 15 h. Next, the suspension was thermally treated at 130 °C for 24 h and cooled to room temperature. The supernatant NaOH solution was discarded and the obtained white powder was suspended in a large amount of distilled water. The dispersion was filtered and re-dispersed in the same quantity of 1 M HCl for 2 h in order to facilitate Na^+ to H^+ exchange. Finally, the formed TiNTs were thoroughly rinsed with deionized water until pH∼6 was reached and dried for 1 h at 100 °C.

TiNTs were stirred in a pure ethanol and toluene (1:1) solution for 1 h. A stock solution of C_{60} in toluene was prepared, and a desired amount of C_{60} was added to the TiNT suspension to reach 1, 2, and 5 wt% C_{60}. The TiNT/C_{60} composite was then agitated for 15 h, filtered, and dried at 80 °C for 5 h. Lastly, the obtained powder was calcined at 350 °C.

2.2. Characterizations

The crystal structure of as-prepared photocatalysts was determined using an X-ray diffractometer (JEOL JDX-3500) operated at 35 kV and 100 mA using CuKα radiation. The UV–vis diffuse reflectance spectra were examined at room temperature with a UV–vis spectrophotometer (UV-2500, Shimadzu). The morphology was observed using a transmission electron microscope (TEM, JEM-2100F, JEOL, Japan) operating at 200 kV. The surface area was measured at 77 K by the conventional Brunauer–Emmett–Teller (BET) method (Gemini 2360, Shimadzu). Raman spectrum measurements were executed using a laser Raman spectrophotometer (Jasco NRS-1000) at room temperature. The power of the incident laser beam was 100 mW with a monochromatic wavelength of 532 nm. The laser pulses were focused onto the surface of the sample with a spot size of approximately 5 μm by using an optical microscope with a 20 × objective lens.

2.3. Photocatalytic activity evaluation

The photocatalytic activity was evaluated from decomposition of gaseous isopropanol (IPA) over the photocatalyst under visible light irradiation. Typically, 0.1 g of the photocatalyst was spread uniformly in a dish with an irradiation area of 7.8 cm^2; the dish was placed on the base of a 500 mL reactor. After the reactor was sealed with a quartz cover and the inside atmosphere replaced with synthetic air, 450 ppm of gaseous IPA was introduced into the reactor. The reactor was stored in the dark until the concentration ceased changing and the system reached the adsorption equilibrium. The reactor was then irradiated with visible light ($\lambda > 420$ nm) that was emitted from a Xe lamp using a cutoff filter (L-42, Hoya Corp., Japan) and a water filter. The concentrations of IPA, acetone, and CO_2 were monitored using a gas chromatograph (GC-14B, Shimadzu Corp., Japan) equipped with a flame ionization detector (FID) and a methanizer.

3. Results and discussion

Fig. 1 shows the SEM images of the sample after hydrothermal processing and acidic rinsing. At low magnification, soft agglomeration granules with typical size of 1–10 μm produced by the vacuum filtering process can be observed. In high-resolution images, one-dimensional nanomaterials up to a few hundred nanometers, with strong agglomeration, can be clearly distinguished [25]. No morphological changes were observed after impregnation with fullerenes.

The TEM image in Fig. 2a represents a TiNT sample loaded with 2 wt% C_{60}. We observed open-ended nanotubes which are several hundred nanometers in length. The inner diameter of TiNT is 3–6 nm, while the outer diameter is about 7–15 nm. When the loading of C_{60} was 1 and 2 wt%, we did not observe any large agglomerates of fullerenes; however a smooth and homogenous distribution of "clusters" was found within the inner and on the outer parts of the TiNTs. From the TEM observation we could estimate an average size of C_{60} clusters between 2 and 5 nm. In contrast to the above results, when loaded with 5 wt% C_{60} we could observe large 20–100 nm agglomerates or assemblies of fullerenes (Fig. 2b). Despite this phenomenon, the interconnection between TiNT and C_{60} still seems strong due to a large proportion of TiNTs embedded in and on the surface of C_{60} agglomerates. To further assess the effect of C_{60} loading and its affinity for TiNTs, EDX analyses were carried out to confirm the presence of C_{60} within TiNTs matrix agglomerates. For the sample without any addition of

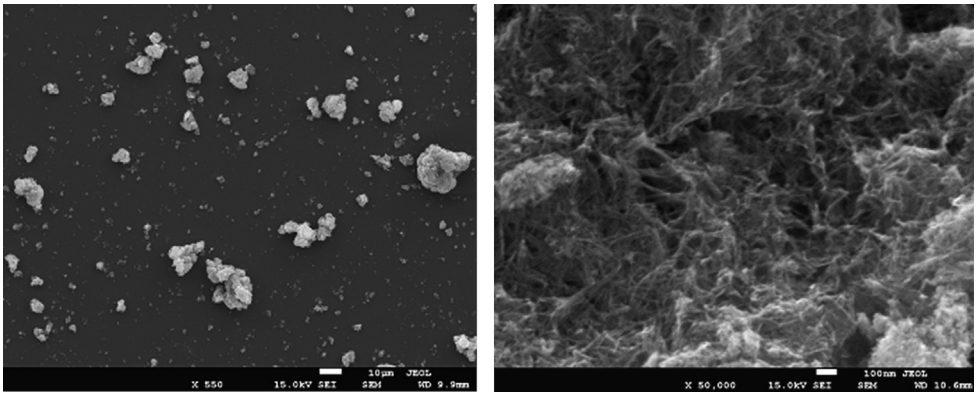

Fig. 1. SEM images of the sample after hydrothermal reaction and acidic rinsing showing strong agglomeration of one-dimensional nanomaterials.

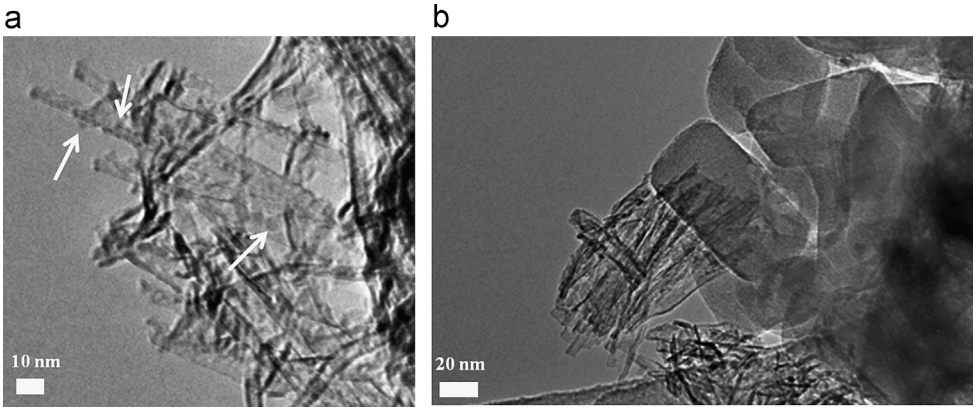

Fig. 2. TEM images of (a) TiNT C_{60} 2 wt% and (b) TiNT C_{60} 5 wt%.

C_{60}, i.e. TiNTs only, a carbon signal has been attributed to contamination in the analysis chamber. For samples with low C_{60} loading (1 and 2 wt%), the ratio of Ti Kα to C Kα peaks is significantly higher when compared with pristine TiNTs, which indicates the presence of carbonaceous compounds in the TiNT matrix. All samples confirmed the following typical spectrum features: (i) a zone where large aggregates of C_{60} are present (i.e. 5% C_{60}), showing a large carbon signal along with the presence of titanium and, (ii) zones where TiNTs aggregate (i.e. 1% and 2% C_{60}) with a relatively high signal of carbon compared to pristine TiNTs. The mode of interaction between TiNTs and C_{60} is directly related to the mechanism of photooxidation, and can be related to the work of Kamat et al. [26]. Authors showed that the photoejection of electrons into titania is likely to be followed by the interaction of fullerene radical $C_{60}^{\bullet+}$ with either the lattice or chemisorbed oxygen that results in the formation of an epoxide type species, suggesting strong bonding on titania surface.

The Raman scattering spectrum of pure TiNTs in Fig. 3a features several Raman bands at 185, 270, 448, 669, 835, and 928 cm^{-1}, which can be ascribed to TiNTs [27]. For 1 and 2 wt% C_{60} samples, the detection of specific bands for C_{60} was not possible probably due to the detection limit of the apparatus. However, we observed a slight enhancement in Raman band intensities of titania due to the calcinations process at 350 °C. Nevertheless, for 5 wt% C_{60} with TiNTs, some characteristic bands were observed as shown in Fig. 3b at 271.5, 493.5, 1421.5, 1464.5, and 1565.5 cm^{-1}. These bands arise from large fullerene-based clusters formation in the suspension. Importantly, Raman spectra measurement showed a Raman band at 1464.5 cm^{-1}, corresponding to A_g pentagonal pinch modes, which indicates that C_{60} clusters retain pristine monomeric C_{60} molecules [28]. The arrangement of large fullerene clusters is here arisen from weak interactions, such as Van der Waals forces, between C_{60} molecules.

XRD patterns of pure C_{60} crystals and TiNT-C_{60} 5% are shown in Fig. 4. The XRD pattern of as-received pure C_{60} presented a spectrum that showed several diffraction intensities in good agreement with the literature for pristine fullerenes C_{60} [29]. The XRD pattern of titania signals in the TiNT C_{60} 5% sample was fundamentally the same as those reported previously for TiNTs, presenting four major peaks at 24.5°, 38.0°, 48.4°, and 54.7° [30]. A peak at 2θ~14° (a typical peak for layered titanates corresponding to interlayer distance) was small and broad, which indicates that crystallinity of TiNTs was relatively poor. However, the nanotubes structure is typical of short-term and low-temperature hydrothermal treatment. Additional diffraction peaks were detected at 39.8°, 46.3°, and 67.5°, which correspond to C_{60} formed aggregates and apparently show enough C_{60} grown to be detected, although in a crystalline form different than its original structure. One can note the conservation of a similar peak at 67.5° between pristine and as-synthesized C_{60} agglomerates, and the

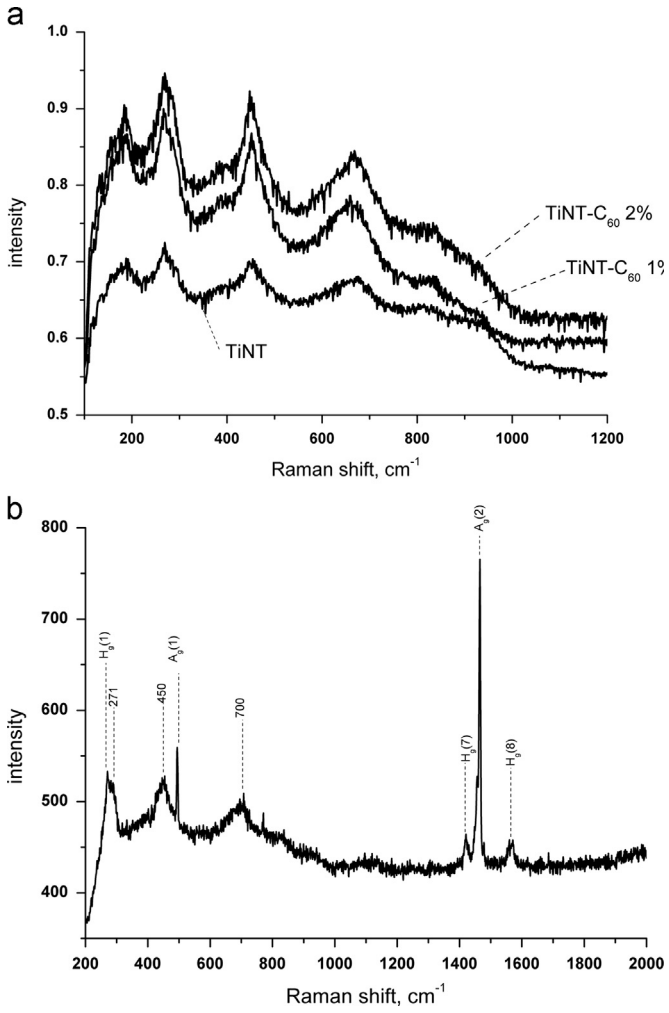

Fig. 3. Raman spectra of (a) pristine TiNT and samples loaded with 1 and 2 wt % of C_{60} (b) detailed spectrum of TiNT C_{60} 5 wt%.

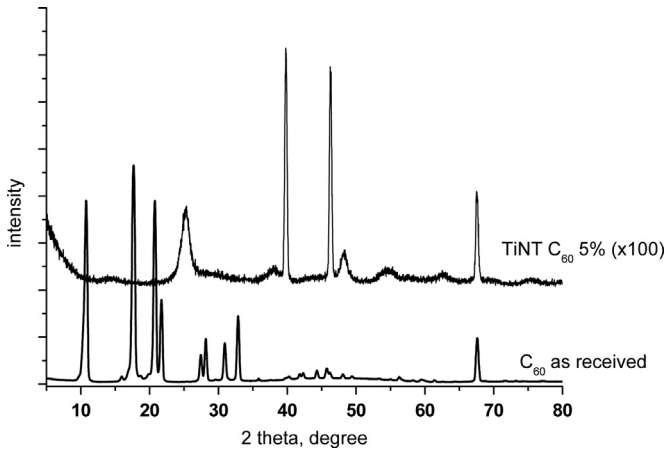

Fig. 4. XRD pattern of pure C_{60} crystals (as-received) and TiNT-C_{60} 5 wt% (intensity × 100).

poor relative intensity of the C_{60} peaks compared before and after synthesis i.e. *relative intensity of signals* × 100.

Previous work showed the formation of supramolecular nanomaterials with different shapes like fibers, cones and discs

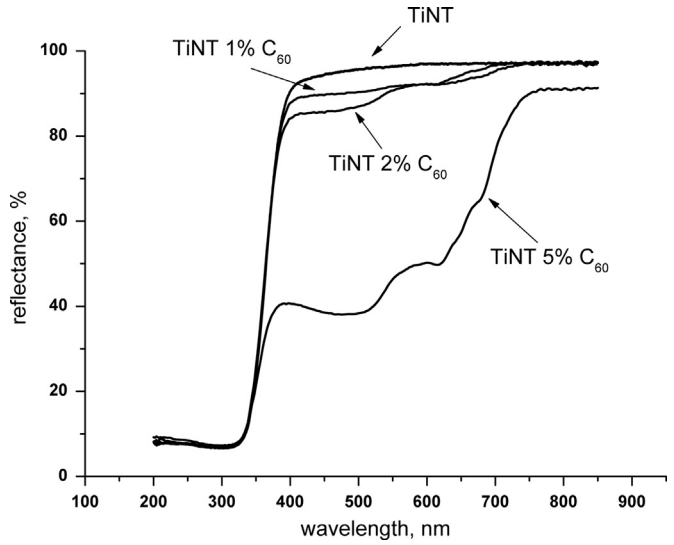

Fig. 5. UV–vis spectra of titania nanotubes impregnated with 1, 2 and 5 wt% of C_{60} and compared to pristine TiNT.

based on the self-assembly of fullerene derivatives with long alkali chains in solvents like isopropanol:toluene [31]. Miyazawa et al. showed similar Raman profiles with pure C_{60} in a mixture of organic solvents using the so-called liquid–liquid interfacial precipitation LLIP method [32]; however, we conducted our experiment under agitation and not in static mode. In the case of static mode, fullerene nanotubes, nanowires or even nanopellets can be grown and could possibly be investigated in the future. For this study, it is believed that the formation of C_{60} clusters during the synthesis under agitation occurred by a supersaturated state of C_{60} enhanced by the addition of alcohol.

The diffuse reflectance absorption spectra of the different mass ratios of C_{60}-hybridized TiNTs samples are presented in Fig. 5. The major strong absorption around 380 nm comes from the TiNTs. However, we observe visible absorbance for all C_{60}-TiNT composite samples in the visible region from 400 to 800 nm. Three different absorption bands were identified at 500, 620, and 680 nm, which correspond to the absorption of fullerene aggregates. Recently, Long et al. suggested that the introduction of C_{60} into TiO_2 nanorods enhances a higher absorption in the 400–800 nm range due to electronic interactions between C_{60} and TiO_2 [33]. Under UV-A irradiation, the photogenerated electrons may transfer to C_{60}, which is favorable to the enhancement of the photocatalytic activity. One can observe the great enhancement of visible light absorption for the sample at 5 wt%, which has been attributed to the formation of large C_{60} clusters.

The photocatalytic activity of TiNT/C_{60} nanostructures was evaluated by isopropanol (IPA) mineralization, a common model compound, under visible light irradiation. IPA, along with other alcohols, is also a major contaminant within indoor air and air stream [34]. Under dark testing, the concentration of IPA went to zero and no CO_2 formation was detected. No catalytic process was observed, while the rapid concentration diminution occurred due to IPA adsorption onto the powder

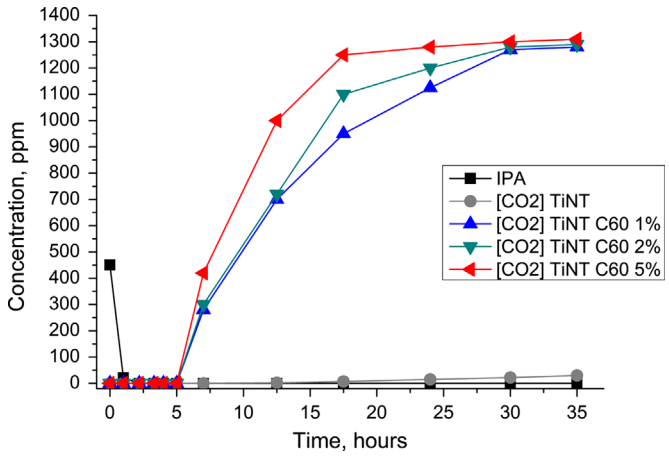

Fig. 6. Photocatalytic activity of C_{60}-sensitized titania nanotubes samples towards IPA degradation under visible light irradiation and compared to pristine TiNT. IPA concentration (■) was zero and CO_2 formation was monitored during all photocatalytic tests.

with high specific surface area. Under visible light irradiation, gaseous IPA was gradually oxidized through an acetone intermediate to CO_2. The concentration of acetone in the system during all experiments was very low and therefore we only focused on the evolution of CO_2 during our experiments. The concentration changes of IPA and CO_2 versus time are shown in Fig. 6.

It is clear that nearly no photocatalytic activity was observed when pristine TiNTs were used as a catalyst, owing to a large band gap (3.5 eV) and therefore no visible light absorption. We did not detect any IPA during this test because of the high adsorption of IPA onto TiNT due to its large specific surface area. A pure C_{60} sample was also tested and demonstrated no photocatalytic activity for IPA mineralization under visible light.

TiNTs loaded with 1 and 2 wt% of C_{60} showed similar results with a complete mineralization of IPA in about 20 h. Among all photocatalysts, TiNT-C_{60} 5% demonstrated the best activity for degradation of IPA under the present conditions with complete mineralization in 11 h. Therefore, the photocatalytic performance of TiNTs can be drastically improved in the visible region by the addition of C_{60} for the mineralization of isopropanol.

There are different factors influencing the photocatalytic activity of such composite material. According to the literature, fullerene C_{60} solid is a narrow band semiconductor with a direct band gap of 1.6–1.9 eV. The band gaps of TiNTs and C_{60} are ideally positioned so that upon visible light photoexcitation, the C_{60} complexes promote interfacial electron injection into the TiNT conduction band host substrate, leading to electron/hole separation. This photosensitization process has therefore a double role of visible light harvesting and injection of photogenerated electrons into the TiNTs photocatalyst. The specific surface area of the samples was also found to be high with typical values around 290 m^2/g, which is obviously beneficial for surface reactions. A decrease in specific surface area between raw TiNTs and C_{60}-TiNT samples calcined at 350 °C has been observed, suggesting the formation of a dense tunnel structure as proposed in previous work [35] and which is in agreement with TEM observations.

4. Conclusions

In summary, we have successfully synthesized TiNTs and C_{60} composites from a facile process. The evolution of the C_{60} concentration in solution during synthesis was crucial for the formation of large clusters, offering a drastic enhancement in the visible range absorption and in photocatalytic activity. When TiNTs were loaded with 5 wt% of C_{60}, we observed the best photocatalytic activity. The enhanced photocatalytic activity under visible light has been attributed to (i) an effective separation of photoexcited electron/hole pairs, thus sensitization with C_{60} and (ii) a high specific surface area.

Acknowledgments

This work was supported by the International Center for Young Scientists (ICYS), National Institute for Materials Science (NIMS), Tsukuba, Japan. The authors are thankful to Dr. A.S. Torralba for the graphical abstract, M. Frank and Dr. J. Williams for their precious help.

References

[1] M. Kaneko, K. Okura, Photocatalysis: Science and Technology, Springer, New York, 2002.
[2] X. Sun, Y. Li, Synthesis and characterization of ion-exchangeable titanate nanotubes, Chemistry: A European Journal 9 (2003) 2229.
[3] H. Tokudome, M. Miyauchi, Electrochromism of titanate-based nanotubes, Angewandte Chemie International Edition 44 (2005) 1974.
[4] H. Tokudome, M. Miyauchi, Titanate nanotube thin films via alternate layer deposition, Chemical Communications (2004) 958.
[5] H. Tokudome, M. Miyauchi, N-doped TiO_2 nanotube with visible light activity, Chemistry Letters 33 (2004) 1108.
[6] S.M. Liu, L.M. Gan, L.H. Liu, W.D. Zhang, H.C. Zeng, Synthesis of single-crystalline TiO_2 nanotubes, Chemistry of Materials 14 (2002) 1391.
[7] M.A. Correa-Duarte, L.M. Liz-Marzan, Carbon nanotubes as templates for one-dimensional nanoparticle assemblies, Journal of Materials Chemistry 16 (2006) 22.
[8] G. Gundiah, S. Mukhopadhyay, U.G. Tumkurkar, A. Govindaraj, U. Maitra, C.N.R. Rao, Hydrogel route to nanotubes of metal oxides and sulfates, Journal of Materials Chemistry 13 (2003) 2118.
[9] V. Zwilling, E. Darque-Ceretti, A. Boutry-Forveille, D. David, M. Y. Perrin, M. Aucouturier, Structure and physicochemistry of anodic oxide films on titanium and TA6V alloy, Surface and Interface Analysis 27 (1999) 629.
[10] T. Kasuga, M. Hiramatsu, A. Hoson, T. Sekino, K. Niihara, Formation of titanium oxide nanotube, Langmuir 14 (1998) 3160.
[11] T. Kasuga, M. Hiramatsu, A. Hoson, T. Sekino, K. Niihara, Titania nanotubes prepared by chemical processing, Advanced Materials 11 (1999) 1307.
[12] R. Ma, Y. Bando, T. Sasaki, Nanotubes of lepidocrocite titanates, Chemical Physics Letters 380 (2003) 577.
[13] G.H. Du, Q. Chen, R.C. Che, Z.Y. Yuan, L.M. Peng, Preparation and structure analysis of titanium oxide nanotubes, Applied Physics Letters 79 (2001) 3702.
[14] J. Yang, Z. Jin, X. Wang, W. Li, J. Zhang, S. Zhang, Z. Guo, Z. Zhang, Study on composition, structure and formation process of nanotube $Na_2Ti_2O_4(OH)_2$, Dalton Transactions (2003) 3898.

[15] Z. Wu, F. Dong, W. Zhao, H. Wang, Y. Liu, B. Guan, The fabrication and characterization of novel carbon doped TiO_2 nanotubes, nanowires and nanorods with high visible light photocatalytic activity, Nanotechnology 20 (2009) 235701.
[16] M. Grandcolas, A. Louvet, N. Keller, V. Keller, Layer-by-layer deposited titanate-based nanotubes for solar photocatalytic removal of chemical warfare agents from textiles, Angewandte Chemie International Edition 48 (2009) 161.
[17] H.-C. Liang, X.-Z. Li, Visible-induced photocatalytic reactivity of polymer-sensitized titania nanotube films, Applied Catalysis B 86 (2009) 8.
[18] B.O. Reagan, M. Gratzel, A low-cost, high-efficiency solar cell based on dye-sensitized colloidal TiO_2 films, Nature 353 (1991) 737.
[19] Q. Li, Z. Jin, Z. Peng, Y. Li, S. Li, G. Lu, High-efficient photocatalytic hydrogen evolution on eosin Y-sensitized Ti-MCM41 zeolite under visible-light irradiation, Journal of Physical Chemistry C 111 (2007) 8237.
[20] P. Fu, Y. Luan, X. Dai, Preparation of activated carbon fibers supported TiO_2 photocatalyst and evaluation of its photocatalytic reactivity, Journal of Molecular Catalysis A 221 (2004) 81.
[21] D. Wang, D. Choi, J. Li, Z. Yang, Z. Nie, R. Kou, D. Hu, C. Wang, L. V. Saraf, J. Zhang, I.A. Aksay, J. Liu, Self-assembled TiO_2–graphene hybrid nanostructures for enhanced Li-ion insertion, ACS Nano 3 (4) (2009) 907.
[22] G.K.R. Senadeera, V.S.P. Perera, Photoresponses of a photovoltaic cell prepared by CuSCN electrodepositing C_{60} on mesoporous TiO_2, Chinese Journal of Physics 43 (2) (2005) 384.
[23] P.V. Kamat, I. Bedja, S. Hotchandani, Photoinduced charge transfer between carbon and semiconductor clusters. one-electron reduction of C_{60} in colloidal TiO_2 semiconductor suspensions, Journal of Physical Chemistry 98 (1994) 9137.
[24] V.I. Makarov, S.A. Kochubei, I.V. Khmelinskii, Photoconductivity of the TiO_2+fullerene-C_{60} bilayers: steady-state and time-resolved measurements, Chemical Physics Letters 355 (2002) 504.
[25] Y. Suzuki, B. Pichon, M. Grandcolas, N. Keller, V. Keller-Spitzer, S. Yoshikawa, Preparation and microstructure of titanate nanotube thin films by spray layer-by-layer assembly method 1. Agglomerate problem of titanate nanotubes for thin-film processing, Transactions of Materials Research Society of Japan 34 (3) (2009) 545.
[26] P.V. Kamat, M. Gevaert, Photochemistry on semiconductor surfaces. Visible light induced oxidation of C_{60} on TiO_2 nanoparticles, Journal of Physical Chemistry B 101 (1997) 4422.
[27] T. Gao, H. Fjellvag, P. Norby, Crystal Structures of titanate nanotubes: a Raman Scattering study, Inorganic Chemistry 48 (2009) 1423.
[28] H.S. Shin, S.M. Yoon, Q. Tang, B. Chon, T. Joo, H.C. Choi, Highly selective synthesis of C_{60} disks on graphite substrate by a vapor–solid process, Angewandte Chemie International Edition 47 (2008) 693.
[29] M. Sathish, K. Miyazawa, J.P. Hill, K. Ariga, Solvent engineering for shape-shifter pure fullerene (C_{60}), Journal of the American Chemical Society 131 (2009) 6372.
[30] J. Yu, H. Yu, B. Cheng, C. Trapalis, Effects of calcination temperature on the microstructures and photocatalytic activity of titanate nanotubes, Journal of Molecular Catalysis 249 (2006) 135.
[31] T. Nakanashi, W. Schmitt, T. Michinobu, D.G. Kurth, K. Ariga, Hierarchical supramolecular fullerene architectures with controlled dimensionality, Chemical Communications (2005) 5982, http://dx.doi.org/10.1039/B512320H.
[32] K. Miyazawa, Thesis and properties of fullerene nanowhiskers and fullerene nanotubes, Journal of Nanoscience and Nanotechnology 9 (2009) 41.
[33] Y. Long, Y. Lu, Y. Huang, Y. Peng, Y. Lu, S.-Z. Kang, J. Mu, Effect of C_{60} on the photocatalytic activity of TiO_2 nanorods, Journal of Physical Chemistry C 113 (2009) 13899.
[34] W. Xu, D. Raftery, Photocatalytic oxidation of 2-propanol on TiO_2 powder and TiO_2 monolayer catalysts studied by solid-state NMR, Journal of Physical Chemistry B 105 (2001) 4343.
[35] E. Morgado Jr., M.A.S. de Abreu, G.T. Moure, B.A. Marinkovic, P. M. Jardim, A.S. Araujo, Effects of thermal treatment of nanostructured trititanates on their crystallographic and textural properties, Materials Research Bulletin 42 (2007) 1748.